Insulated Supply for Semiconductor Placed at High Voltage Potentials in a Marx Generator

F. Lopes[1], H. Canacsinh[2], L. M. Redondo[2,*]

[1]Lisbon Engineering Superior Institute, ISEL, Lisbon, Portugal

[2]Pulsed-Power Advanced Applications Group, Lisbon Engineering Superior Institute, GIA[2]P[2]/ISEL, Lisbon, Portugal

[*]E-mail: lmredondo@deea.isel.ipl.pt

Abstract **-** The purpose of this paper is to analyze a topology of a series resonant converter based on an inverter with an LC series resonant circuit and a transformer with multiple isolated secondaries to supply power to the high voltage IGBTs trigger circuits in each Marx generator stage. This paper deals with the analysis, simulation, and design of the series resonant converter. It shows that through the accommodating the leakage inductances of the transformer the converter has a good performance. Experimental and simulation results are presented with load variations on the driver side, resistive load on Marx Generator and a severe situation were caused on driver circuit to makes it fail. This kind of converter could be used on Marx generator, induction heat [1], satellite power supply, pulsed power supply for radars [2], automotive batteries charger, contactless power transfer system [3] and others.

Keywords **-** LC Series resonant converter; Inverter; Full-bridge; Marx Generator; Pulsed power; ZVS; ZCS; Leakage Inductance.

I. INTRODUCTION

The continuous development of power semiconductors, allowed them to switch higher powers, enabling the evolution of pulsed power in stack topologies, namely the Marx generator, based on semiconductors type IGBTs or MOSFETs, which can operate normally up to about 1kV.

The Marx generator is a circuit where various capacitors are charged in parallel from a relatively low dc power supply, U_{dc}, and then subsequently these capacitors are connected in series with a load in order to generate high-voltage pulses in the order of kVs, with μs pulse width and repetition rate, as seen in Fig. 1, using semiconductor switches. Because of this operation, it is mandatory that the trigger electronics of the semiconductor devices are isolated galvanically, which poses some challenges in supplying energy to these circuits that are at high potentials, namely the galvanic isolation to high voltage and immunity to electromagnetic interference.

In Fig. 1 is an example of a 3-stage positive Marx generator based on MOSFET type semiconductors switches [4]. Where S_2, S_4, S_6 and S_7 are *on* during capacitor charging, and then S_1, S_3 and S_5 are *on* during pulse to the load Z_L.

There are several techniques used to produce an isolated voltage to supply energy to the semiconductor trigger electronics in Marx generator stages that support the high potentials, among which there is the topology presented in this paper, the resonant LC series converter, based on a DC- AC type Full-Bridge with an LC series circuit at its output and placed in series with the primary winding of the transformer.

This feeding method, although more complex than the bootstrap method, for example, allows the regulation and isolation of the output voltage [5].

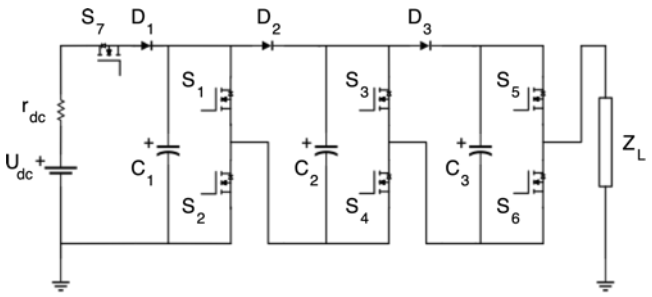

Fig. 1. Simplified positive 3 stage Marx generator circuit.

However, the use of the transformer, which makes it possible to isolate and adjust the output voltage, causes some problems for inverter switching due to leakage inductances of the high-frequency transformer, in which the inverter has what is called hard switching, producing high switching losses [6].

By using a LC series circuit between the inverter output and the primary winding of the transformer to absorb the leakage inductances of the high-frequency transformer, enables the operation at the resonant frequency, where the capacitive reactance cancels out the inductive reactance, which results in a purely resistive circuit, at the resonant frequency f_r, with maximum gain. In this situation, the inverter will operate in so-called soft switching.

For the converter to be able to operate at the resonant frequency, it is necessary to measure the leakage inductance of the transformer L_r, set the switching frequency f_s, set the normalized frequency $F = 1$ and define the quality factor Q based on the load resistance. Taking these, it is possible to determine the capacitance of the series resonant capacitor C_r.

The normalized frequency F is defined by:

$$F = \frac{f_s}{f_r} \tag{1}$$

In Fig. 2 is presented the Gain vs normalized frequency graphic for LC series resonant converter, where it can be possible to observe that at $F = 1$ the gain will be maximum.

Also, it is possible to observe the operation regions, described by ZCS- Zero Current Switching and ZVS- Zero Voltage Switching. The ZCS mode is obtained when the converter operates with $f_s < f_r$, and when the converter operates at $f_s > f_r$ the converter enters on ZVS region.

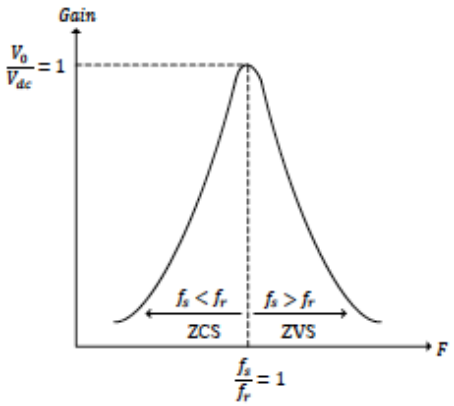

Fig. 2. Gain vs normalized frequency graphic for LC series resonant converter.

In this type of converter if neglecting the transformation ratio of the transformer the maximum gain is equal to the unity.

The circuit design, computational calculation, simulation, and practical implementation were performed, the results are discussed, thus validating the benefits of this topology.

The laboratory prototype consists of the series resonant converter, with the Full-Bridge inverter based on MOSFETs, with LC series resonant circuit and the transformer composed by 1 primary winding and 4 secondary windings, in which each secondary feeds 2 stages of the Marx generator of the laboratory, totaling 8 stages, having 4 stages per PCB. Each stage of the Marx generator can operate up to 1kV, totalizing 8kV of impulse voltage at the output of Marx's generator.

II. CIRCUIT TOPOLOGY

Fig. 3 presents the resonant converter topology of the series LC circuit with transformer and multiple independent secondary and control the IGBT drivers of the Marx generator stages, where V_{dc} is the input voltage and V_0 is the output voltage of the converter.

The transformer is composed by 4 toroidal cores, secondary windings being independent and only primary winding running through the 4 toroidal cores.

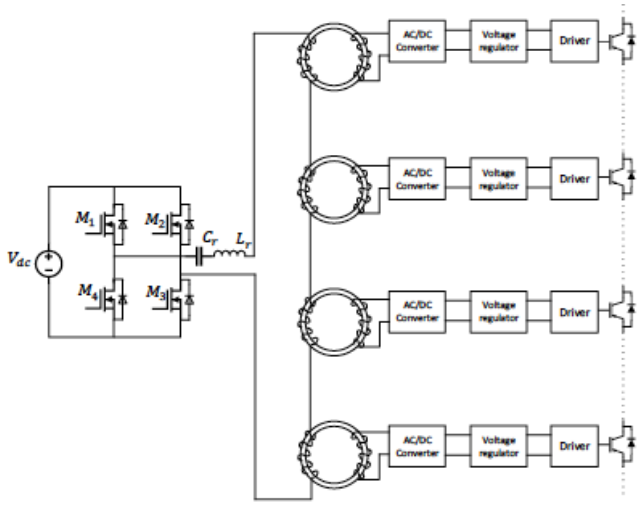

Fig. 3. LC series resonant converter circuit connected to the trigger circuits of the Marx generator stages semiconductors

The capacitor C_r is the resonant capacitor, and L_r is the leakage inductance. The MOSFET pairs M_1-M_3 and M_2-M_4 switch with the full-wave command, that is, in pairs with a some short dead time between the *on-off* transitions, thus obtaining the voltage waveform and current according to Fig. 4 [7].

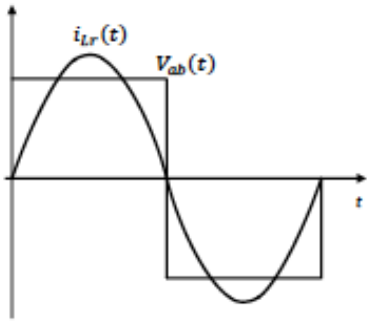

Fig. 4. Voltage and current waveforms of the full-wave command

It can be assumed that the set of the linear voltage regulator and the driver of each secondary can be simplified as a resistive-capacitive (RC) load, and the AC-DC converter composed of a diode rectifier bridge. Thus, in Fig. 5 a simpler and more exact diagram of the converter and its load is obtained.

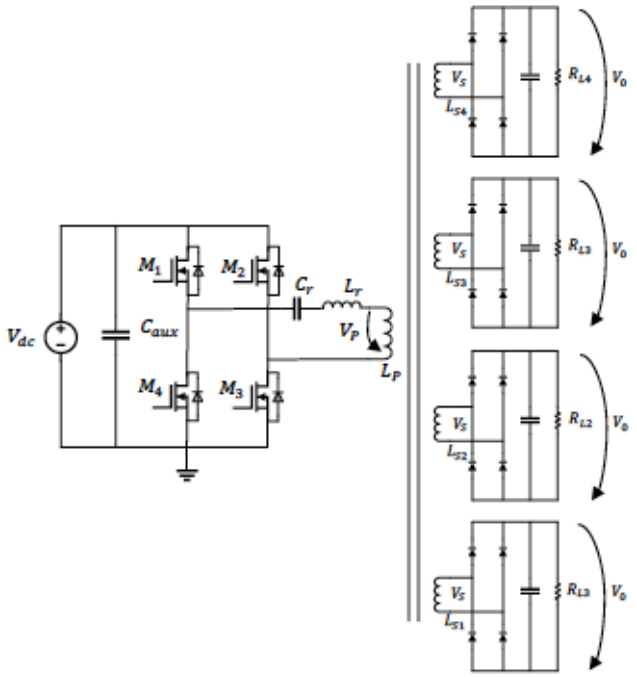

Fig. 5. Resonant circuit with 4 secondaries and 8 stages of Marx generator

In Fig. 5, V_P is the voltage applied to the primary winding of the transformer and the coil L_P is the inductance of the primary winding. The voltage V_S applied to the secondary is equal in all the secondary windings being given by eq. (2), where n is the transformer ratio of the transformer:

$$V_S = \frac{V_P}{n} \tag{2}$$

Also, L_{S1}, L_{S2}, L_{S3}, L_{S4} and R_1, R_2, R_3, R_4 are the inductances of the windings and the load resistances of the secondaries, respectively. The voltage V_0 is the voltage applied to the loads, after rectification.

Although the secondary windings are composed by the same type of elements, it can be simplified for design purposes and ideally it is possible to put an equivalent circuit as shown in Fig. 6, where $R_L{}'$ is the equivalent resistance of all secondary side view of the primary [2].

$$R_L{}' = \frac{R_{L\,equiv.}}{\left(\frac{N_S}{N_P}\right)^2} \tag{3}$$

where $R_{L\,equiv}$ is the equivalent resistance of all secondary, and N_P and N_S are the turn numbers of the primary and secondary windings, respectively.

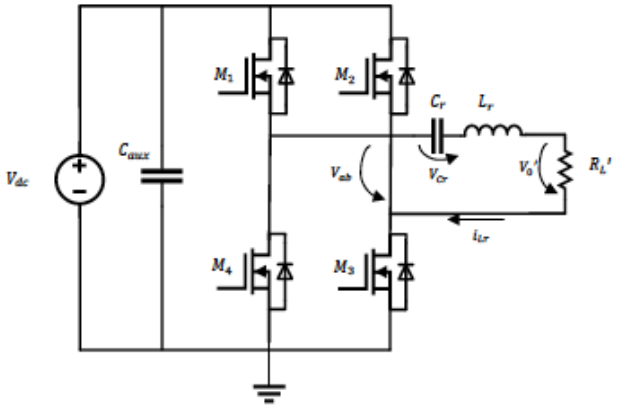

Fig. 6. Equivalent circuit with secondary load resistance reduced to the primary

The maximum amplitude of the square wave voltage at the output of the inverter V_{ab} is equal to its RMS value, and neglecting the voltage drops in the semiconductors, can be considered as $V_{ab} = V_{dc}$. The resonant capacitor voltage V_{Cr}, and its maximum amplitude V_{Crpk} is determined by,

$$V_{Crpk} = \frac{i_{Lrpk}}{2\pi f_r C_r} \tag{4}$$

where i_{Lrpk} is the maximum amplitude of the resonant circuit current i_{Lr}. The design of the resonant circuit is defined by the quality factor Q and the normalized frequency F. And the quality factor Q can be determined by

$$Q = \frac{Z_0}{R_L{}'} \tag{5}$$

The characteristic impedance Z_0 is defined by :

$$Z_0 = \sqrt{\frac{L_r}{C_r}} \quad (6)$$

Since f_s is the switching frequency of the inverter and f_r is the resonant frequency, and can be obtained by :

$$f_r = \frac{1}{2\pi\sqrt{L_r C_r}} \quad (7)$$

III. EXPERIMENTAL RESULTS

Fig. 7 shows the experimental prototype of the LC series resonant converter of Fig. 3, that was built with a transformer with 4 independents secondaries, where each secondary feeds 2 IGBTs drivers from the Marx generator. In the experimental tests, each stage produced 125V, adding to 1kV of pulse voltage at the output of the Marx generator. Fig. 8 shows the Marx generator with 4 secondaries.

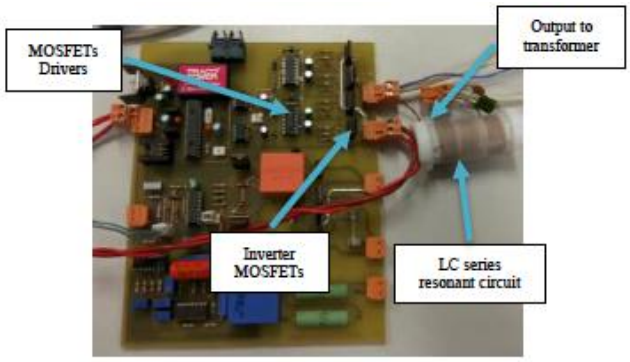

Fig. 7. Prototype of LC series resonant converter

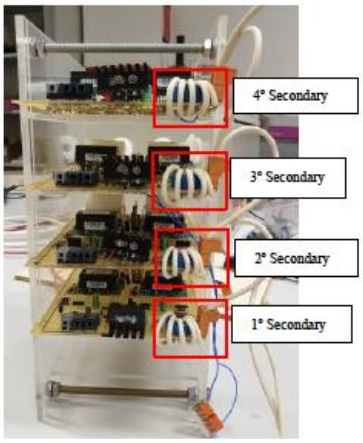

Fig. 8. Transformer secondaries of Marx generator

Table I presents the operation parameters and the components of the converter obtained in the design.

In Table I, the switching frequency of the inverter f_s, the equivalent load referred to the primary $R_L{}'$ are calculated through eq. (3), in which the load of a secondary was obtained through the measurement during operation with $V_S = 20$ V.

The DC voltage of the power supply V_{dc} is about 15V, and the voltage V_{ab} at the output of the inverter is 13.3V, in order to produce a voltage of 20V on each secondary, which is the voltage supply of the trigger circuits.

Table I - Parameters

$R_L{}'$	14.14 Ω
V_{ab}	13.3 V
L_r	23 µH
C_r	124 nF
f_s	95.3 kHz
f_r	94 kHz
F	1.01
Q	2.16

The quality factor Q has been defined as 2.16, to obtain a current sinusoidal waveform without increasing the current that circulates in the resonant circuit, and also increases the voltage of the resonant capacitor V_{C_r} as shown in eq. (4), which may not be feasible [8].

As mentioned previously, the purpose of the converter operation would be around $F = 1$, more precisely $f_s = f_r$, but due to the difficulty of having the exact value of the components for this operating point, it was chosen tan operating slightly above f_r, that is $f_s > f_r$.

This mode of operation is known as Zero Voltage Switching (ZVS) and is preferred when using MOSFETs in the inverter because it mitigates the switching losses caused by the output capacity of these semiconductors. After these definitions, it is then possible to determine f_r, L_r, and C_r.

Fig. 9 and Fig. 10 present the results obtained by simulation and by the experimental test with the optical-fibers of the trigger control signals connected to the semiconductor drivers.

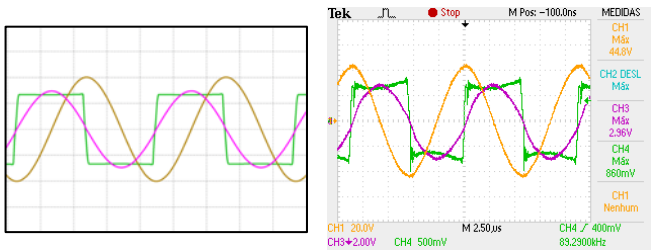

Fig. 9. Waveforms of V_{ab}, i_{Lr}, V_{Cr}, obtained by: (left) simulation; (right) experimental test: 2.5µs/div; (green) V_{ab}, 10V/div; (brown) V_{Cr}, 20V/div; (pink) i_{Lr}, 2A/div

It is observed from Fig. 9 the waveforms of the inverter output voltage with an amplitude of $V_{ab} \approx$

$13V$, the current in the resonant circuit with an amplitude of $i_{Lr} \approx 3A$ and the resonant capacitor voltage with an amplitude of $V_{Cr} \approx 40V$.

Fig. 10 shows the voltage at the output of the inverter V_{ab}, with an amplitude $V_{ab} \approx 13V$, the current in the resonant circuit i_{Lr} with an amplitude of $i_{Lr} \approx 3A$ and the voltage V_S of the 4th transformer secondary with an amplitude of $V_S \approx 20V$).

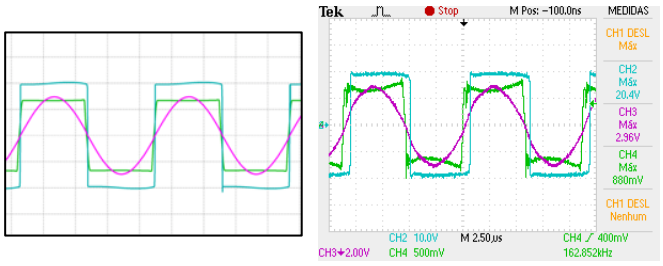

Fig. 10. Waveforms of V_{ab}, i_{Lr}, V_S, obtained by: (left) simulation; (right) experimental test: 2.5µs/div; (green) V_{ab}, 10V/div; (blue) V_S, 20V/div; (pink) i_{Lr}, 2A/div

In Fig. 11 a) and Fig. 11 b) present, respectively, the results obtained by experimental tests without and with the command signals of the drivers.

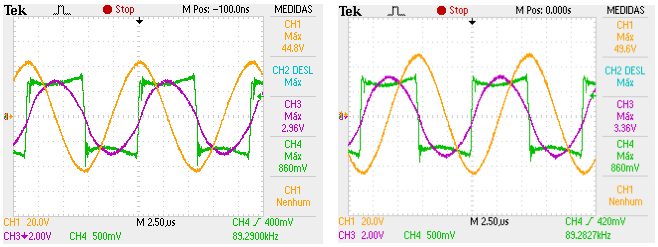

Fig. 11. Waveforms of V_{ab}, i_{Lr}, V_{Cr}, obtained by experimental test: (left) without command signals (right) with command signals: 2.5µs/div; (green) V_{ab}, 10V/div; (brown) V_{Cr}, 20V/div; (pink) i_{Lr}, 2A/div

The waveforms of the voltage at the output of the inverter $V_{ab} \approx 13V$, of the current in the resonant circuit $i_{Lr} \approx 3{,}4A$ in Fig. 11 a), and in b) with an amplitude of $i_{Lr} \approx 3A$. This difference in the amplitude of i_{Lr} is due to the internal operation of the optocoupler, consuming more current in the absence of fiber-optic signals. The resonant capacitor voltage $V_{Cr} \approx 50V$ and $V_{Cr} \approx 40V$ in Fig. 11 a) and b) are also observed respectively. It is verified that the voltage V_{Cr} it's directly proportional to the current i_{Lr}, as already demonstrated in eq. (4).

Fig. 12 shows the results obtained by the experimental test with a voltage pulse $V_{Pulse} \approx 1kV$ applied at the resistive load of 500 Ω at the output of the Marx generator.

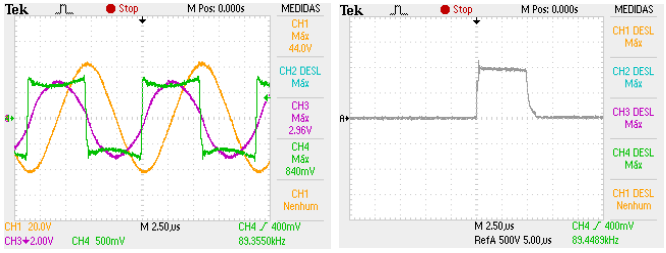

Fig. 12. Waveforms of: (left) (green) V_{ab}, 10V/div; (brown) V_{Cr}, 20V/div; (pink) i_{Lr}, 2A/div; (right) V_{pulse}, 500V/div. 2.5µs/div

The waveforms of the voltage at the output of the inverter $V_{ab} \approx 13V$, the current in the resonant circuit $i_{Lr} \approx 3A$, and the voltage in the resonant capacitor $V_{Cr} \approx 40V$, and the voltage of the pulse $V_{Pulse} \approx 1kV$ are shown in Fig. 13.

Fig. 13 show the experimental test under adverse conditions consisted of causing an anomaly in the IGBT gate control driver, leading to IGBT operation and protection, cutting the command signal to an IGBT of the 8th stage of power, in the 4th secondary of the transformer.

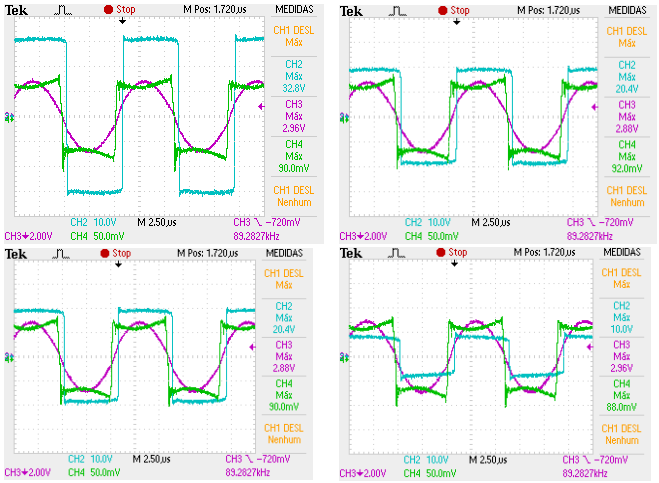

Fig. 13. Waveforms of V_{ab}, i_{Lr} and V_S for experimental testing in adverse conditions obtained by: (a) 4th secondary, (b) 3rd secondary, (c) 2nd secondary, and (d) 1st secondary. 2.5µs/div; (green) V_{ab}, 10V/div; (blue) V_S, 20V/div; (pink) i_{Lr}, 2A/div

The objective was to understand the impact that this type of anomalies of the Marx in the resonant converter.

This adverse condition causes the two secondary windings of the transformer to be unbalanced, i.e. the 4th secondary with a further 10V being with a voltage $V_{S4} \approx 30V$ and the 1st secondary with less 10V, being with a voltage $V_{S1} \approx 10V$, while in normal operation they would have a voltage $V_S \approx 20V$.

At the time of this occurrence, the IGBT's gate control circuit protects itself by turning itself off, drastically reducing the current in the secondary where the severe condition occurs. Since the voltage of the primary winding V_P remains unchanged, the voltage of the 4th secondary V_{S4} increases and the voltage of the 1st secondary V_{S1} decreases.

By decreasing the voltage of the 1st secondary V_{S1}, the current of this secondary increase, in order to maintain the same power delivered to the load resistance (IGBT driver), causing the current i_{Lr}, which circulates in the primary winding, unchanged from normal operation.

Comparing the values of the simulation and the experimental part, both have a good agreement, and their differences are due to the simplifications used in the simulation.

IV. CONCLUSIONS

A resonant LC series converter with an independent secondary transformer used to feed the semiconductor control drivers of the stages of the Marx generator, which are at high voltage potential, has been analyzed.

Conceptually the proposed topology, resonant LC converter series with transformer, is an optimized version of the inverter PWM with a transformer on the output, which allows having greater yield through the soft commutations that increase the life of the devices of the converter.

It can be concluded that can be possible to reduce switching losses with this circuit, taking advantage of the presence of the leakage inductances of the several toroidal transformers, and also very stable since the primary side circuit of transformer is not affected by the resistive load variations of the Marx generator.

In the case of the test with an adverse condition in Fig. 13, it is verified that the increase of 10V in the 4th secondary can compromise the supply of the control circuit of the stages if they are not adequately protected against surges.

The values of the simulation and experimental part have both a good agreement, and their differences are due to the simplifications used in the simulation.

V. REFERENCES

[1] A. Namadmalan, "Universal Tuning System for Series-Resonant Induction Heating Applications," *IEEE Trans. Ind. Electron.*, vol. 64, no. 4, pp. 2801–2808, 2017.

[2] N. Vishwanathan, "DC to DC Converter Topologies for High Voltage Power Supplies Under Pulsed Loading," no. February. 2004.

[3] Cong Zheng *et al.*, "High-Efficiency Contactless Power Transfer System for Electric Vehicle Battery Charging Application," *IEEE Journal of Emerging and Selected Topics in Power Electronics*, vol. 3, no. 1. pp. 65–74, 2014.

[4] L. M. S. Redondo, "Pulsed Power Fundamentals (semiconductor based technology)."

[5] H. Canacsinh, L. M. Redondo, and J. F. Silva, "Isolated autonomous capacitive power supplies to trigger floating semiconductors in a marx generator," *IEEE Int. Symp. Ind. Electron.*, no. May 2014, pp. 821–826, 2007.

[6] M. H. Rashid, *Power Electronics Handbook*. 2007.

[7] J. F. Silva, *Eletrónica de Potência*, 2nd ed. Fundação Calouste Gulbenkian, 2013.

[8] Robert W. and D. M. Erickson, *Fundamentals of Power Electronics*. 2002.